Geochemical Journal, Vol. 26, pp. 261 to 277, 1992

Trace elements and Nd–Sr isotopes of island arc tholeiites from frontal arc of Northeast Japan

SHIGEKO TOGASHI[1], TSUYOSHI TANAKA[1], TAKEYOSHI YOSHIDA[2], KEN-ICHI ISHIKAWA[2], AKIHIKO FUJINAWA[3] and HAJIME KURASAWA[1]

Geological Survey of Japan, Tsukuba, Ibaraki, 305[1],
Faculty of General Education, Tohoku University,
Sendai, Miyagi, 980[2], and
Faculty of Science, Ibaraki University,
Mito, Ibaraki, 310[3], Japan

(Received March 1, 1991; Accepted August 21, 1992)

On the basis of trace element abundances and Sr and Nd isotope ratios, Quaternary island arc low-alkali tholeiites(IAT) in Northeast Japan are divided into two types; U(undepleted)- and D(depleted)-IAT.

U-IAT are characterized by high and constant abundances of Large Ion Lithophile Elements(LILE), which are 10–20 times higher than the primitive mantle value. The range of Nd isotope ratios of U-IAT is identical within errors to the Bulk Earth value. The $^{87}Sr/^{86}Sr$ ratios of U-IAT range from 0.7047 to 0.7057, greater than or equal to the currently accepted Bulk Earth value, and these variations can be caused by initial heterogeneity in Rb/Sr ratios of the primitive mantle. It is argued that U-IAT magmas were derived by 5–10% batch partial melting of the primitive mantle.

D-IAT are characterized by convex-upward patterns with a maximum normalized value for an alkaline earth element in a primitive mantle versus ionic radii(NPR) abundance diagram. The degree of depletion in the elements with larger ionic radii is greater than those with smaller ones. These characteristics cannot be explained by magma compositional variations derived by different degrees of partial melting of a homogeneous mantle or by fractional crystallization. They can rather be explained by a variation in the composition of a previously depleted mantle source. The isotopic compositions of Sr and Nd range from the value of the Bulk Earth to that of the most depleted oceanic island basalt, and are well correlated with Nb/Y ratios. A mantle isochron of about 1 Ga is obtained for Nd and Sm isotopes. D-IAT magmas are considered to have formed in two stages consisting of depletion in LILE and Nb due to a loss of an extremely small amount of melt (<1%), about 1 Ga from a primitive mantle, and more recently followed by 5–10% partial melting episode under the conditions of formations typical of the U-IAT magmas.

INTRODUCTION

Some island arc basalts (IAB) resemble N-type mid-oceanic ridge basalts (N-MORB) more closely than any other terrestrial basalt type in terms of REE (Rare Earth Elements), Th and U concentrations, and La/Yb, Th/U and K/Rb ratios. However, they differ from N-MORB in their higher concentrations of alkalis and alkaline earths, and lower concentrations of Zr, Hf, Nb and Ta. In addition, they typically have slightly higher concentration ratios of $^{87}Sr/^{86}Sr$ and $^{207}Pb/^{204}Pb$ at a specific $^{206}Pb/^{204}Pb$, and lower $^{143}Nd/^{144}Nd$ than do N-MORB (Jakeš and Gill, 1970; Perfit *et al.*, 1980; Kay, 1980; Gill, 1981).

There are several controversial hypotheses regarding the genesis of IAB. Jakeš and Gill (1970) and a number of other authors (Nicholls and Ringwood, 1973; Nakamura *et al.*, 1985; Arculus and Powell, 1986, Perfit and Kay, 1986; Sakuyama and Nesbitt, 1986) have suggested that the composition of IAB can be explained by the mixing of partial melts or aqueous fluids

derived from the resorbed subducted oceanic lithosphere and the overlying upper mantle. On the other hand, Arculus and Johnson (1981) have suggested that the addition of subducted material to the mantle wedge above the descending slab is not very important because there is not a positive correlation between the magnitude of Sr enrichment and $^{87}Sr/^{86}Sr$ ratios in most island arc rock suites. Instead, they proposed that the contamination of magma by feldspar-bearing lower crust with low $^{87}Sr/^{86}Sr$ ratios is a more important process. In broad terms, this concept has been endorsed at least for the Andes by Hildreth and Moorbath (1988) and central and southwest Japan by Matsuhisa and Kurasawa (1983). This process, however, does not easily explain the restricted chemical composition of IAB in comparison with the reported variety of lower crustal materials. Morris and Hart (1983, 1986) and Stern and Ito (1983) demonstrated that the concentrations of LILE (Large Ion Lithophile Elements) in the source of IAB is similar to that of Oceanic Island Basalts (OIB). These authors think that the similarity is a serious problem for any model invoking addition of subducting materials to the mantle wedge (Tatsumi *et al.* 1986).

For a precise discussion of the composition of the mantle wedge, low-alkali tholeiite (Kuno, 1966) is the best material to be investigated, because it represents the largest partial melt of the mantle source (Sakuyama and Nesbitt, 1986). The concentration ratios of LILE in low-alkali tholeiite magmas are then comparable to those in the mantle source. This implies that it is possible to discuss the composition of the mantle source through the analysis of low-alkali tholeiite features.

A large volume of low-alkali tholeiites has erupted along the volcanic front of Northeast Japan. Previous studies have considered the Sr isotopes (Notsu, 1983), Nd and Sr isotopes (Nohda and Wasserburg, 1981) O-isotopes (Matsuhisa, 1979) and trace element geochemistry (Masuda and Aoki, 1979; Yoshida and Aoki, 1984; Sakuyama and Nesbitt, 1986) of Quaternary arc lavas from Northeast Japan.

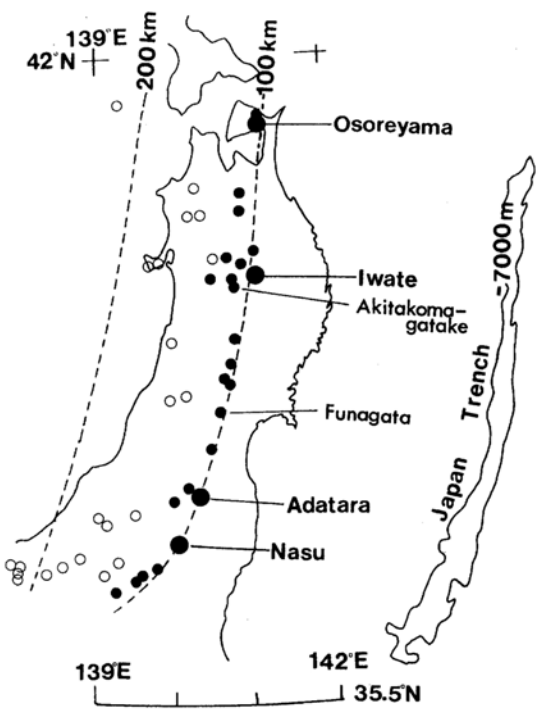

Fig. 1. Index map of Quaternary volcanoes in Northeast Japan. Solid circles: fore-arc side volcanoes, open circles: back-arc side volcanoes, dashed lines: contour of Wadati-Benioff plane.

However, these studies failed to integrate isotope and elemental data on the same samples.

The purpose of this paper is to present a new genetic model for the tholeiites from Northeast Japan and their source mantle in the light of trace element concentrations and Nd–Sr isotope ratios consistently obtained for the same samples. The compositions of IAT are explained by partial melting of primitive mantle or residual mantle after a prior loss of a small amount of melt.

Samples, Analytical Methods and Results

Samples were collected from the Osoreyama, Iwate, Adatara and Nasu volcanoes along the Quaternary volcanic front of Northeast Japan (Fig. 1). The least differentiated rocks of the magma series in each volcano were selected to minimize the effects of fractional crystallization or other secondary processes. In some cases,

Table 1. Major and trace element contents in rocks from the volcanoes on the Quanternary volcanic front of NE Japan

		Iwate				Nasu			
	type	U	U	D	D	U	U	U	U
sample No.		IWA7	IWA10	IWA36	IWA41	8561601	8561603	8580205	8580403
No. for Fig. 5		I1	I2	I3	I4	N1	N2		
SiO_2	g*	52.84	53.42	51.09	50.19	53.17x	53.14x	61.96x	57.99x
TiO_2	c	0.83	0.80	0.78	0.80	0.79x	0.81x	0.65x	0.70x
Al_2O_3	g	18.40	18.21	18.23	19.33	18.01x	18.35x	15.86x	16.56x
Fe_2O_3	g	3.27	3.52	2.22	2.64	10.33x	10.19x	7.44x	8.70x
FeO	g	6.24	5.76	7.55	7.09				
MnO	c	0.15	0.16	0.16	0.19	0.17x	0.16x	0.13x	0.15x
MgO	g	4.38	5.23	6.91	6.17	4.94x	4.72x	3.32x	4056x
CaO	g	9.87	9.90	10.68	10.57	10.16x	10.11x	6.76x	7.89x
Na_2O	a	2.35	2.15	1.96	2.14	1.98x	2.05x	2.61x	2.29x
K_2O	a	0.39	0.37	0.15	0.19	0.35x	0.31x	1.27x	0.81x
P_2O_5	g	0.11	0.11	0.30	0.07	0.09x	0.10x	0.07x	0.08x
H_2O^+	g	0.53	0.33	0.04	0.45				
H_2O^-	g	0.20	0.14	0.09	0.46				
Total		99.56	100.10	100.16	100.29	99.99	99.94	100.07	99.73
Cs	p	1.34		1.17	0.04				
Rb	i	9.3	9.1		1.2	7.66	6.37	40.5	30.1
K	a	3240	3070	1250	1580	2900x	2520x	10500x	6700
Na	a	17400	15900	14500	15800	14700x	15200x	19300x	16900
Ba	i	129		621	61.9	134		318x	213
Sr	i	288n	308n	293n	283n	278	277	201	230x
La	i	6.20	4.6n	2.0n	2.43	6.36		10.6n	6.58
Ce	i	13.18	12.6n	5.2p	6.11	12.61		23.8n	15.4
Nd	i	7.34			4.57	7.07			8.30
Sm	i	2.00	1.8n	1.3n	1.46	2.03		3.3n	2.30
Eu	i	0.752	0.7n	0.53n	0.634	0.722		0.83n	0.737
Gd	i	2.41			2.02	2.49			2.83
Dy	i	2.59			2.16	2.75			2.98
Er	i	1.64			1.40	1.75			1.90
Yb	i	1.62	1.3n	1.1n	1.35	1.74		2.7n	1.96
Lu	i	0.256	0.2n	0.15n	0.205	0.265		0.4n	0.296
Y	p	16.1	19.3	12.3	13.2	16.1x		25.6x	20.4x
Hf	n	1.1	1.2	0.19				3.13	
Zr	p	50.5	50.0	24.8	24.2	41.2x		111x	71.1x
Ti	c	4980	4800	4680	4800	4740x	4860x	3900x	4200x
Th	n	1.06	1.12	0.32				4.1	
U	n			0.07				1.1	
Nb	p	3.2	4.2	1.1	2.1				
SrI		0.70474	0.70468	0.70432	0.70427	0.70488	0.70495	0.70527	0.70525
NdI		0.51269	0.51271	0.51281	0.51288	0.51269	0.51269	0.51268	0.51271

	type	Osore				Adatara			
		D	D	D	D	D	U	D	D
sample No.		OSO1	OSO9	OSO14	OSO28	2-1	2-2	3-1	3-3
No. for Fig.5		O1				A1	A2		
SiO_2	g*	53.12	65.58	57.95	61.79	51.99	53.14	55.92	57.28
TiO_2	c	0.79	0.58	0.61	0.47	1.02	1.04	0.97	0.95
Al_2O_2	g	19.19	16.30	16.78	16.87	20.37	18.37	17.13	16.68
Fe_2O_3	g	2.54	2.79	3.89	3.39	4.02	4.79	4.27	4.00
FeO	g	6.63	3.25	4.68	3.81	5.07	5.19	5.53	4.90
MnO	c	0.18	0.12	0.14	0.16	0.15	0.16	0.14	0.14
MgO	g	4.48	1.38	3.72	2.64	3.77	4.53	4.06	3.44
CaO	g	9.80	5.06	8.00	6.47	9.79	8.59	7.04	7.49
Na_2O	a	2.27	3.13	2.18	3.28	2.39	2.54	2.42	2.57
K_2O	a	0.25	0.66	0.49	0.54	0.28	0.40	1.17	1.24
P_2O_5	g	0.14	0.12	0.11	0.10	0.21	0.20	0.16	0.18
H_2O_+	g	0.50	0.56	0.50	0.29	0.50	0.47	0.58	0.55
H_2O_-	g	0.09	0.37	0.37	0.11	0.25	0.37	0.33	0.23
Total		99.98	99.90	99.42	99.92	99.81	99.79	99.72	99.65
Cs	p	0.081	0.35	0.17	2.13	0.16		0.41	0.39
Rb	i	3.3	16.4	13.4	12.8	3.2p	9.6p	32.1p	35.2p
K	a	2080	5480	4070	4480	2520	3600	10500	10300
Na	a	16800	23200	16100	24300	17700	18800	17900	19000
Ba	i	100	267	165I	230I	107	132	272	274
Sr	i	262x	219x	212x	197x	299	275	245	231
La	i	3.17	9.61	4.30	5.0n	6.22		9.61	
Ce	i	8.03	20.2	11.04	11.9n	14.03	15.1p	21.66	17.6p
Nd	i	5.96	12.3	6.65		9.61		12.13	
Sm	i	1.93	3.55	2.08	2.2n	2.76		3.22	
Eu	i	0.76	1.08	0.738	0.80n	0.980		0.927	
Gd	i	2.58	4.60	2.79		3.54		3.80	
Dy	i	2.98	5.29	3.34		3.64		4.09	
Er	i	1.95	3.57	2.28		2.28		2.63	
Yb	i	1.93	3.60	2.32	2.2n	2.13		2.57	
Lu	i	0.299	0.533	0.379	0.4n	0.323		0.406	
Y	p	19.7	41.0	22.6	21.6	22.0	25.9	25.9	27.3
Hf	n				1.8				
Zr	p	33.6	82.0	42.0	52.8	52.3	74.6	94.1	101
Ti	c	4740	3480	3660	2820	6120	6240	5820	5700
Th	n	0.4γ			1.0γ				
U	n								
Nb		0.81	2.6	1.2	1.0	4.9	4.8	4.0	4.9
SrI		0.70381	0.70415	0.70388	0.70385	0.70571	0.70552	0.70500	0.70515
NdI		0.51286	0.51288	0.51292	0.51297	0.51266	0.51268	0.51273	0.51276

The analytical method used most for a given element is given at the second column; exceptions are identified.

* *abbreviations of analytical methods.*

g; gravimetry, c; colorimetry, a; atomic absorption method, p; photon activation analysis (Electron Linac of Nuclear Science, Tohoku Univ., Yoshida et al., 1986), i; isotope dilution method using mass spectrometer, I; inductively coupled plasma-optical emission spectrometry (by N. Onuma), n; neutron activation analysis, x; X-ray fluorescence, γ; γ-ray spectrometry (with assumption of radiometrical equilibrium, K. Sato and J. Sato, unpublished data).

Iwate Volcano: Data from Ishikawa (1993) except for Nd isotope ratios and trace element data measured by mass spectrometer. Sample descriptions: IWA7; Augite bearing olivine bronzite andesite, somma lava of the Older Iwate Volcano. IWA10; Olivine bearing aguite-bronzite andesite, somma lava of the Older Iwate Volcano. IWA36; Olivine basalt, lava of Yakushidake cone, the Younger Iwate Volcano. IWA41; Bronzite-olivine basalt, lava of Myokodake cone, the Younger Iwate Volcano.

Nasu Volcano: Sample description: 8561601; Olivine-bearing augite-hypersthene andesite, Numappara lava, the Older Nasu Volcano. 8561603; Olivine-bearing augite-hypersthene andesite, Numappara lava, the Older Nasu Volcano. 8580205; Olivine-bearing augite-hypersthene andesite, Akatsura lava, the Older Nasu Volcano. 8580403; Olivine-augite-hypersthene andesite, Chausu lava, the Younger Nasu Volcano.
Osoreyama Volcano: Sample description: OSO1; Olivine-augite-hypersthene andesite, Kamabuseyama lava. OSO9; Augite-bearing hypersthene dacite Kitaguniyama lava. OSO14; Augite-hypersthene andesite, T-1 lava. OSO28; Augite bearing hornblende-hypersthene andesite, Tsurugiyama lava.
Adatara Volcano: Data from Fujinawa (1989) for major and trace elements and from Kurasawa et al. (1986) for Sr isotope ratios. Sample description: 2-1; Olivine-augite bearing hypersthene andesite, Maegatake-nishi lava, the second stage. 2-2; Augite-hypersthene andesite, Akagidaira lava, the second stage. 3-1; Olivine bearing augite-hypersthene andesite, Yakushidake lava, the third stage. 3-3; Olivine-bearing augite-hypersthene andesite, Adatarayama lava, the third stage.

more differentiated rocks were also analyzed to evaluate the effects of fractional crystallization. A brief petrographic description of the samples is presented in the footnote of Table 1.

Analytical methods for major and trace element determinations are indicated in Table 1. Typical analytical errors for major elements are less than 2%, those for Cs and Nb are up to 30% because of very low contents, those for Hf, Th and U are less than 10%, and those for other trace elements are less than 5%. The isotopic compositions of Sr and Nd were determined with an automated mass spectrometer with double collectors (VG-Micromass 54E). The measured $^{86}Sr/^{88}Sr$ ratios were normalized to 0.1194 to correct the $^{87}Sr/^{86}Sr$ ratios for instrumental fractionation and then the corrected values were renormalized to a value of 0.70800 for the E and A standard; 2σ errors for the $^{87}Sr/^{86}Sr$ ratios were less than 0.00004. The measured $^{146}Nd/^{144}Nd$ ratios were normalized to 0.72190 in order to correct the $^{143}Nd/^{144}Nd$ ratios for instrumental fractionation. The normalized value of our measurement for LaJolla standard was 0.511848 ± 24 (2σm), and all reported values have been renormalized to 0.511859 for the LaJolla standard (Lugmair and Carlson, 1978). The normalized value for BCR-1 is 0.512629 ± 20 (2σm) and that for JB-1 (a geostandard rock of GSJ) is 0.512798 ± 26 (2σm).

The results are presented in Table 1. Major element data show that all the analyzed samples belong to the low-alkali tholeiite series (Kuno, 1966), and low-K or medium-K series (Gill, 1981). These rocks are characteristically enriched in LILE and depleted in high field strength elements (HFSE) relative to N-MORB and belong to the IAB type of Perfit, *et al.* (1981). Hereafter, we refer to these rocks as island arc tholeiites (IAT).

Two Types of Island Arc Tholeiite

The Normalized Abundance against Primitive Mantle diagram (NAP), according to the normalization reported in Nakamura *et al.* (1985), is effective for the study of the genesis of magmas related to the N-MORB source (see Table 2 for various sets of normalizing values). In the NAP diagram, the order of the elements on the horizontal axis is arranged according to their degree of incompatibility, which is estimated on the basis of the concentration ratio particularly between N-MORB and the primitive mantle. The NAP diagram for IAT (Fig. 2) has a saw-toothed pattern and is not systematic. In addition, when plotting the N-MORB normalized values against ionic radii, a similar pattern with strong Ba enrichment in both IAT and OIB is observed (Fig. 3). It is difficult to explain the enrichment of LILE in OIB with the recent inevitable addition of subducting materials to the N-MORB source, although it is possible to think the eventual contribution of recycled old subduction materials (White and Hofmann, 1982).

In Figs. 4, 5 and 6, the concentrations of cations in the rock normalized to their abundances in the primitive mantle are plotted against ionic radii. This plot is termed the Normalized abundances against Primitive mantle versus ionic Radii (NPR) diagram. Ionic radii used in the NPR diagram are taken from Shannon

Table 2. Major and trace element abundances in the primitive mantle, C1 chondrite, N-MORB and OIB and their ionic radii

V	E	CN	IR	PM this study	PM Sun & Mc-Donough (1989)	PM Wood *et al.* (1979)	C1 chondrite	N-MORB Sun & Mc-Donough (1989)	OIB Wood *et al.* (1979)
1	Cs	12	1.88	0.073	0.0079	0.019	0.29 a	0.007	0.04
	Rb	12	1.73	0.71	0.635	0.86	2.82 a	0.56	5.2
	K	8	1.51	205	250	252	816 b	600	2840
	Na	8	1.16	1895			7530 b	16650 e	17600
2	Ba	8	1.42	7.2	6.989	7.56	3.6 c	6.3	80
	Sr	8	1.25	22.8	21.1	23	11.4 c	90	224
3	La	8	1.16	0.76	0.687	0.71	0.378 d	2.5	9.2
	Ce*	8	1.14	1.95	1.775	1.90	0.976 d	7.5	23
	Nd	8	1.12	1.43	1.354	1.29	0.716 d	7.3	
	Sm	8	1.08	0.46	0.444	0.385	0.230 d	2.63	
	Eu**	8	1.07	0.173	0.168		0.0866 d	1.02	1.22
	Gd	8	1.06	0.62	0.596		0.311 d	3.68	
	Dy	8	1.03	0.78	0.737		0.390 d	4.55	
	Er	8	1.00	0.51	0.480		0.255 d	2.97	
	Yb	8	0.99	0.50	0.493		0.249 d	3.05	
	Lu	8	0.97	0.077	0.074		0.0387 d	0.455	
	Y	8	1.02	4.2	4.55	4.87	2.1 c	28	20
	Sc	6	0.745	15.6			7.8 c		35.1
4	Hf	6	0.71	0.34	0.309	0.35	0.17 c	2.05	2.30
	Zr	6	0.72	11.4	11.2	11	5.7 c	74	113
	Ti	6	0.605	1320	1300	1527	660 c	7600	8520
	Th	8	1.04	0.102	0.085	0.096	0.051 c	0.12	0.65
	U	8	1.00	0.027	0.021	0.027	0.0135 c	0.047	0.19
5	Nb	6	0.64	0.90	0.713	0.62	0.45 c	2.33	12

*Abbreviations: V; valency states, E; elements, CN; coordination states, IR; Ionic radii (Shannon and Prewitt, 1969, 1970), PM; primitive mantle. Data from a: Krahenbüuhl et al. (1973), b: Nichporuk and Moore (1974), c: Taylor (1980), d: Masuda et al. (1973), e: Frey (1974). *: sometimes tetravalent, **: sometimes divalent. The inferred composition of the primitive mantle, in this work, is estimated from the composition of C1 chondrite (Krahenbuhl et al., 1973; Nichiporuk and Moore, 1974; Taylor, 1980; Masuda et al. 1973 and Frey, 1974) assuming the following enrichment factors of various elements. The enrichment factors relative to C1 for moderately volatile elements such as Cs, Rb, K, Na are assumed to be 0.25 based on Rb/Sr in Nd–Sr isotopic systematics of DePaolo and Wasserburg (1976a). The constant value of the enrichment factors for alkali elements results in the higher content of Cs in our primitive mantle than in others. The enrichment factors for refractory elements such as Ba, Sr, REE, and HFSE are assumed to be 2.0 from Taylor (1980).*

and Prewitt (1969, 1970) on the basis of suitable coordination numbers in the natural states of minerals which constitute the mantle. They are shown in Table 2. The inferred composition of the primitive mantle derived from this study is also shown in Table 2, and compared to the compositions inferred by others. The abundances, with the exception of Cs, are close to other inferred compositions of the primitive mantle (Sun and Nesbitt, 1977; Wood *et al.*, 1979; Sun and McDonough, 1989).

In the NPR diagram for N-MORB (Fig. 4), the pattern is a mirror image of those for IAT and OIB in the NAP diagram (Fig. 3). These facts imply that the depletion of LILE in the N-MORB relative to the primitive mantle causes the apparent enrichment of LILE in both IAT and OIB in the NAP diagram. Also the apparent significant Ba enrichment in both OIB and IAT in N-MORB normalized diagram (Fig. 3) is caused by the significant Ba depletion in N-MORB. On the other hand, the NPR diagram

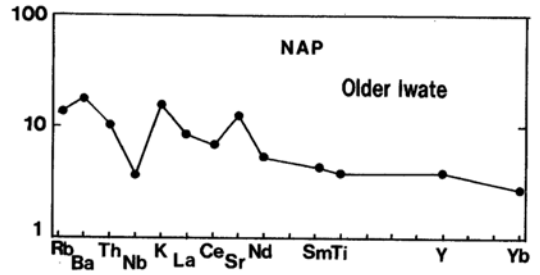

Fig. 2. The NAP disgram (Normalized Abundance against Primitive mantle diagram) for island arc tholeiite (IAT). The NAP diagram is after Nakamura et al. (1985). The concentrations of the elements of rocks are normalized to their estimated abundances in the primitive mantle shown in Table 2. Data for IAT from the Older Iwate volcano are from Table 1.

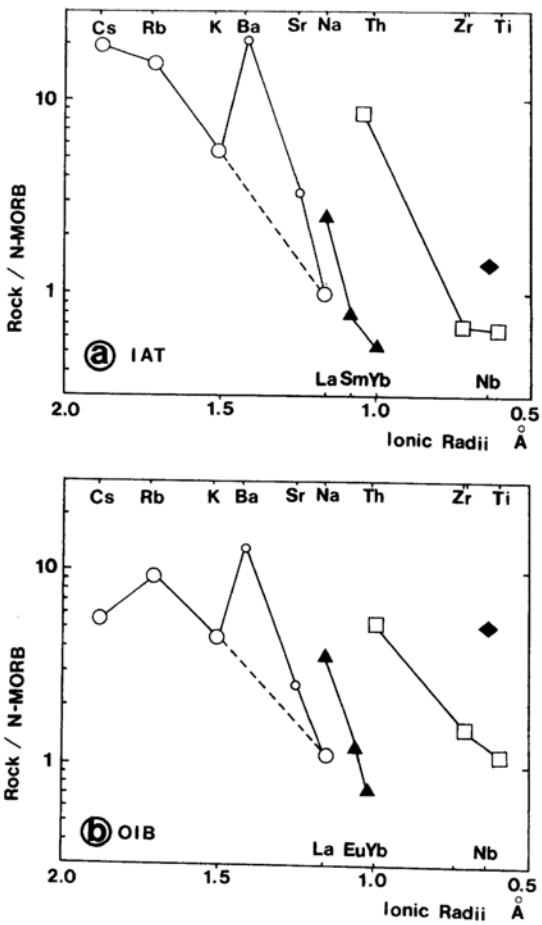

Fig. 3. Normalized abundance against N-type mid-oceanic ridge basalt (N-MORB) vs. ionic radii plot for (a) IAT and (b) oceanic island basalt (OIB). Large open circles:univalent, small open circles:divalent, solid triangles:trivalent, open squares:tetravalent, solid diamonds:pentavalent. Data are from Tables 1 and 2.

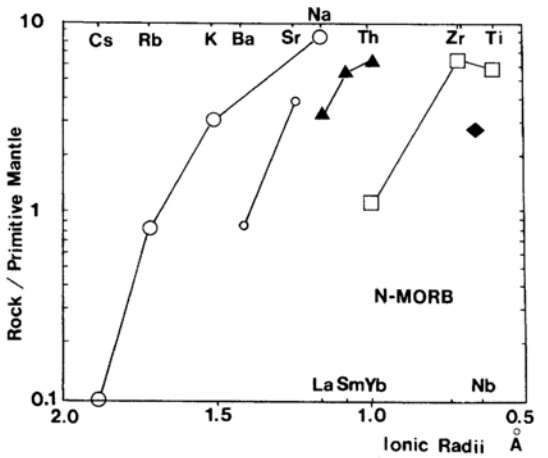

Fig. 4. The NPR diagram (Normalized abundances against the Primitive mantle versus ionic Radii diagram) for N-MORB. Data sources and symbols are the same as in Fig. 3.

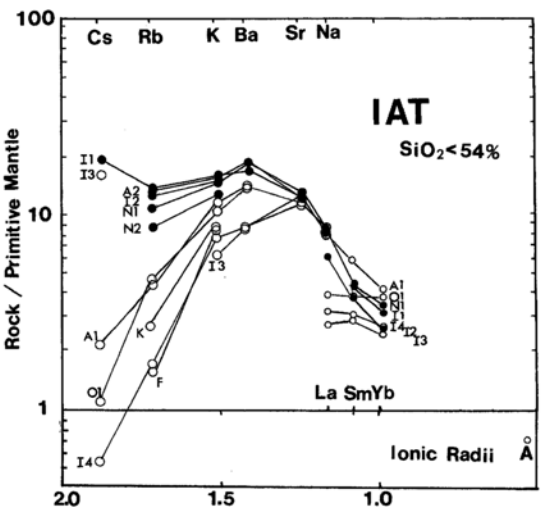

Fig. 5. The NPR diagram for IAT (SiO_2<54%) from Northeast Japan. Data (with letter and No.) are from Table 1, except for K: Akitakomagatake and F: Funagata from Yoshida and Aoki (1984). Solid circles: U-IAT and open circles: D-IAT, large circles:univalent and divalent, small circles: trivalent.

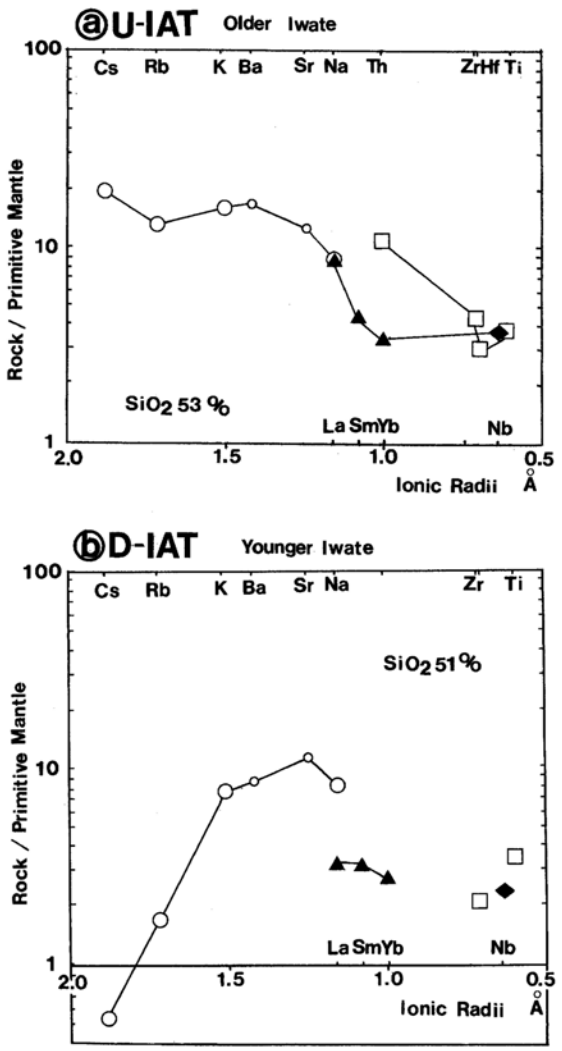

Fig. 6. The NPR diagram for (a) U-IAT and (b) D-IAT. U-IAT from the Older Iwate volcano (IWA7) and D-IAT from the Younger Iwate Volcano (IWA41) are shown in Table 1. Symbols are the same as in Fig. 3.

for IAT shows systematic patterns (Fig. 5). It can, therefore, be concluded that the NPR diagram has a significance for the interpretation of IAT genesis.

The NPR diagram responds to the bulk distribution coefficients of elements which change under variable conditions during magma formation. The horizontal axis of NPR diagram is not fixed by the specific order of the bulk distribution coefficients in contrast with other diagram such as spidergrams. The values of partition coefficients between minerals and liquid are, in fact, vary drastically with the changes of liquid composition, pressure, temperature and P_{H_2O} (Green and Pearson, 1985), and affect the values of the bulk distribution coefficients. Therefore the fixed order of elements based on specific values of the bulk distribution coefficients is questionable. Ionic radii are alternatively chosen as the horizontal axis in the NPR diagram, because the relative values of bulk distribution coefficients between ions are kept systematically against valency states and ionic radii (Matsui *et al.* 1977). Ionic radii and valency states are the significant factors for modifying the positions of variable bulk distribution coefficients of elements in the NPR diagram.

U-and D-IAT in the NPR diagram

In the NPR diagram (Fig. 5), two end members of IAT are recognized-U(undepleted) and D(depleted).

U-IAT

U-IAT are characterized in the NPR diagram by the constant and high normalized values of LILE such as Cs, Rb, K and Ba (10–20 times higher than the abundance in the primitive mantle), and by the decrease of the normalized values of moderate LILE such as Sr, Na and REE with the decrease of ionic radii (Figs. 5 and 6a). The normalized pattern for U-IAT is higher in light REE than in heavy REE (Fig. 6a).

All data currently available on Nd isotopic ratios of U-IAT are close to the value of the Bulk Earth proposed by O'Nions *et al.* (1979) as shown in Fig. 7. On the other hand, the $^{87}Sr/^{86}Sr$ ratios, ranging from 0.7047 to 0.7057, are greater than or equal to the Bulk Earth value (Fig. 7).

D-IAT

D-IAT are characterized by convex-upwards normalized patterns with a maximum value for an alkaline earth element in the NPR diagram (Fig. 5). The normalized values of LILE such as Cs, Rb, K and Ba increase, while those of

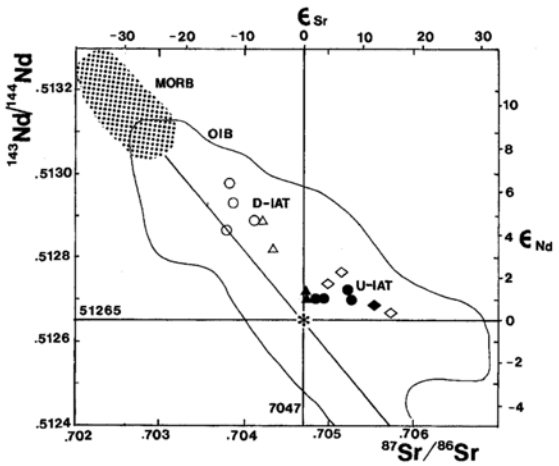

*Fig. 7. Nd and Sr isotopes for U-IAT (solid symbols) and D-IAT (open symbols). Solid and open triangles: Iwate, solid circles: Nasu, solid and open diamonds:Adatara, open circles: Osoreyama, *: Bulk Earth. Data are from Table 1.*

moderately incompatible LILE, such as Sr and Na, decrease with decreasing ionic radii (Figs. 5 and 6b). D-IAT show lower ratio of light REE/heavy REE than those of U-IAT, except for one sample from the Adatara volcano (Fig. 5).

The isotopic compositions of Sr and Nd of D-IAT range between the values of the Bulk Earth and those of depleted OIB (Fig. 7).

Model of Magma Genesis Concerned with the Bulk Distribution Coefficients

The bulk distribution coefficients

The bulk distribution coefficients (D) of elements between magma and solid phase assemblages, which are defined in Table 3, vary not only with temperature, pressure and chemical composition of the system (Green and Pearson, 1985), but also with differences in the mechanism of magma formation.

The mechanism of separation between solid and melt phases seriously affects to the values of the bulk distribution coefficient. The fractional crystallization process is mainly controlled by the mechanical separation of crystals containing melt inclusions from the magma, while the processes involving the separation of melt from the source mantle through partial melting are controlled by the partition coefficient between inclusion-free crystals and magma in a thermodynamic equilibrium.

In the above circumstances, the partition coefficients of incompatible elements between residual mantle and magma are to be significantly lower than those between phenocrysts and magma during fractional crystallization. In fact, the partition coefficients between melt inclusion free clinopyroxenes and melt are low by factors of 6–100 compared to those between melt inclusion bearing clinopyroxenes and melt (Hart and Brooks, 1974). Therefore, it is impossible to use a constant value of D to account for different mechanisms of magma formation.

Models

In the following paragraphs, we will show the effect of the D value on the concentration of an element in a magma derived by Rayleigh fractional crystallization, and in the magma and the residual mantle derived by batch partial melting. Abbreviations are listed in Table 3.

Table 3. List of abbreviation

D=bulk distribution coefficient of element $=(C_A)_S/(C_A)_L$, where C_A denotes oncentration of element A in solid (S) or liquid (L) phase
D′=bulk distribution of the first stage in a two-stage model
D″=that of the second stage in the two stage model
S°=the concentration of an element in the primitive mantle
S′=that in a residual mantle
L°=concentration of an element in an initial magma
L=that in a differentiated magma
L′=that in an initial magma derived from the primitive mantle at the first stage of the two-stage model
L″=that in an initial magma derived from the residual mantle at the second stage of the two stage model
F=degree of fractionation or that of partial melting
F′=degree of partial melting and loss from the primitive mantle at the first stage of the two-stage model
F″=degree of partial melting of the residual mantle at the second stage of the two stage model
Subscripts denote parameters for particular elements (ex. D_{Ba}).

Fractional differentiation

The Rayleigh fractionation process can be expressed by the following eq. (1):

$$\frac{L}{L^\circ}=(1-F)^{(D-1)} \tag{1}$$

When the D values of the two elements (a and b) are smaller than 0.1, the concentration ratio between these elements remains almost constant during Rayleigh fractional crystallization:

$$\frac{L_a}{L_b}\fallingdotseq\frac{L_a^\circ}{L_b^\circ} \tag{2}$$

This holds when the degree of fractional crystallization is less than 90% of the parental magma (Fig. 8a). Thus, small degrees of fractional crystallization do not change the concentration ratio of two incompatible elements having $D<0.1$.

Partial melt

In Fig. 8b, the calculated concentration of an element in magma is shown as a function of D with a parameter of the degree of melting (F) by the following eq. (3):

$$\frac{L}{S^\circ}=\frac{1}{(F+D-F\cdot D)} \tag{3}$$

When two elements have D values smaller than 0.01, such as for Rb, K or Ba, and when the degree of partial melting is larger than 3% such as for tholeiites, the concentration ratio between these elements remains almost constant during the batch partial melting process (Fig. 8b) and can be expressed by the following eq. (4):

$$\frac{L}{S^\circ}\fallingdotseq\frac{1}{F} \tag{4}$$

On the other hand, when the D value of an element is larger than 0.1, such as for Y, the L/S° ratio is approximated to be constant by the following eq. (5), regardless the variation in the F value (Fig. 8b):

$$\frac{L}{S^\circ}\fallingdotseq\frac{1}{D} \tag{5}$$

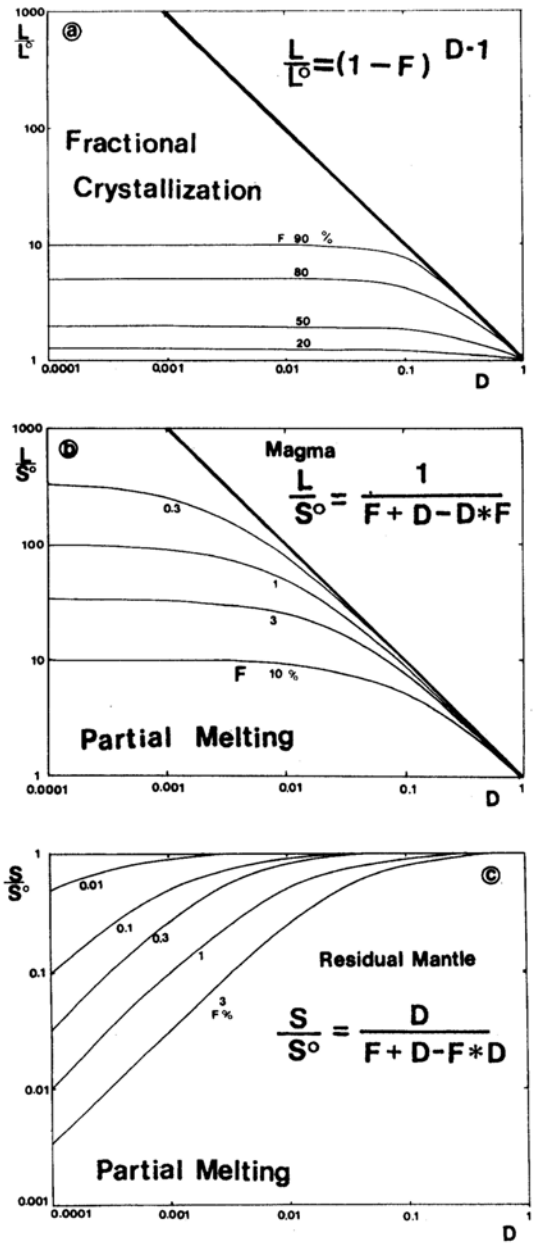

Fig. 8. Variations of concentration ratios of incompatible elements in magma and source mantle against the bulk distribution coefficients (D). (a) differentiated magma during Rayleigh fractional crystailization, (b) magma during batch partial melting. (c) residual mantle during batch partial melting. Abbreviations are shown in Table 3.

Residual mantle

The concentration of incompatible elements in the residual mantle (S) following the separation of the melt from the primitive mantle (S°) can be calculated by using the following eq. (6) for batch partial melting (Fig. 8c):

$$\frac{S}{S^\circ}=\frac{D}{(F+D-F\cdot D)} \tag{6}$$

The S/S° ratio plot in Fig. 8c shows a significantly different pattern from the L/S° ratio plot in Fig. 8b. The S/S° ratio decreases with decreasing D and with increasing degree of partial melting (F), when D is smaller than 0.1, such as for Rb, K or Ba.

Partial melt of the residual mantle (Two-stage model)

During the first stage, a residual mantle is formed by a small degree of partial melting. This process results in the depletion in LILE ($D \ll 0.01$) of the residual mantle (S′) relative to that of the primitive mantle (S°) as shown in eq. (6) and Fig. 8c. During the second stage, the magma (L″) is formed by partial melting of the residual mantle (S′). The concentration of an element in the magma (L″) relative to that of the primitive mantle (S°) is expressed by the following eq. (7):

$$\frac{L''}{S^\circ}=\frac{S'}{S^\circ}\cdot\frac{L''}{S'}=\frac{D'}{(F'+D'-D'\cdot F')}\cdot\frac{1}{(F''+D''-D''\cdot F'')} \tag{7}$$

Figure 9 shows the two-stage model on the assumption of $D'=D''$. Given this assumption, the L″/S° ratio vs. D plot makes a curve convex-upward.

In this model, the L″/S° ratios for moderately incompatible LILE ($D' \geqq 0.01$, $D'' \geqq 0.01$) can be approximately calculated by the following eq.

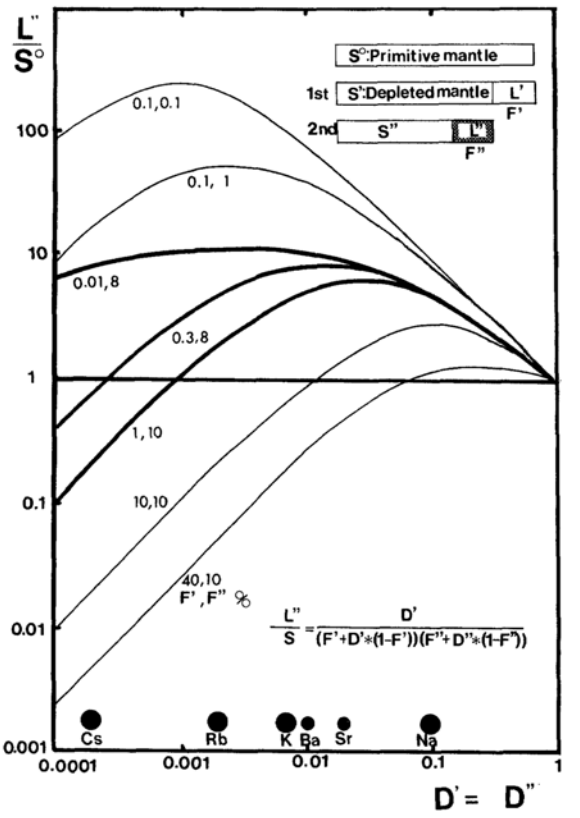

Fig. 9. Two-stage model for D-IAT formation from the primitive mantle. The concentration ratios of magma (L″) to the primitive mantle (S°) are calculated as a function of bulk distribution coefficients (D′ and D″) based on eq. (8). $D'=D''$ is assumed. Abbreviations are shown in Table 3.

(8), when $F'<0.01$ (the undepleted, or slightly depleted residual mantle). Equation (8) is the same formula as eq. (3) for a single-stage partial melting model:

$$\frac{L''}{S^\circ}\fallingdotseq\frac{1}{(F''+D''-D''\cdot F'')} \tag{8}$$

On the other hand, the ratio of D′ between two highly incompatible elements (subscriptions a and b) can be approximated by the following eq. (9), when $D' \leqq 0.01$, $D'' \leqq 0.01$, $F' \geqq 0.003$ and $F'' \geqq 0.05$:

$$\frac{D'_a}{D'_b}=\frac{(L''_a\cdot S^\circ_b)\cdot(F'+D'_a-D'_a\cdot F')\cdot(F''+D''_a-D''_a\cdot F'')}{(S^\circ_a\cdot L''_b)\cdot(F'+D'_b-D'_b\cdot F')\cdot(F''+D''_b-D''_b\cdot F'')}\fallingdotseq\frac{L''_a\cdot S^\circ_b}{S^\circ_a\cdot L''_b} \tag{9}$$

U-IAT Magma Formation from the Primitive Mantle

Basalts of U-IAT from the Iwate and Nasu volcanoes are characterized by constant and high normalized values (10–20 times higher than the primitive mantle value) of LILE such as Cs, Rb, K and Ba (Figs. 5 and 6a). The constant normalized values for LILE indicate that the magma was derived by 5–10% batch partial melting of the primitive mantle and that the values of D of LILE are smaller than 0.01.

The D values of moderately incompatible LILE and HFSE can be calculated from eqs. (3) and (5). The D value of Ba is smaller than 0.01 and that of Sr is 0.02 at 5–10% partial melting calculated on the basis of eq. (3). The D values of La and Na are calculated to be about 0.1 based on eqs. (3) and (5), when the degree of partial melting is less than 10%. To provide such a high D value for La, residual phases where degrees of incompatibility of La and light REE are low are required. The La/Sm ratios of U-IAT (2.2–3.2) are higher than that of the primitive mantle (1.7). This is consistent with that the calculated D for La is smaller than that for Sm, and that both D values are larger than or equal to 0.1 based on eq. (5). The D values of Yb and Y in U-IAT are calculated to be 0.3 on the basis of eq. (5).

In U-IAT, the normalized values of moderately incompatible LILE such as Sr, Na and REE decrease with the decrease in ionic radii on the NPR diagram (Fig. 6a). The similar pattern between Figs. 6a and 8b indicates that the D values of these elements are proportional to the ionic radii regardless of differences in their valency states.

The Nb/Y ratios of U-IAT (0.18–0.23) are constant and similar to the primitive mantle value (0.21), but higher than N-MORB value (0.08)(Fig. 10). On the other hand, the Nb/Y ratios of D-IAT range from 0.04 to 0.23 and are strongly negatively correlate with Nd isotope ratios. This fact is a strong constraint on the composition of the mantle wedge, because the Nb/Y ratio of the source region cannot change by the addition of an aqueous fluid component which contains very small amounts of Nb and Y under the conditions where IAT are formed (Tatsumi *et al.*, 1986). It is a fact that the Nb/Y ratios of magma can be different from that of the source, with a change in F when the D value of Nb is significantly smaller than that of Y (0.3), and when the F value is small (Fig. 8b). But, the F values for IAT and N-MORB are not low. In addition, it is difficult to generate differences by a factor of six in the large F values between N-MORB and U-IAT or among IAT. The uniform Nb/Y ratios in U-IAT show that large changes in Nb/Y ratios do not occur during partial melting. Therefore, the D value of Nb should not be small, but as large as that of Y which is calculated to be 0.3 from eq. (5). Thus, the original mantle wedge of U-IAT could not be a N-MORB-type source, but must be the same as the primitive mantle in terms of relatively high Nb/Y ratios.

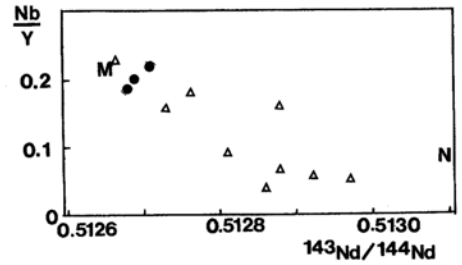

Fig. 10. Nb/Y ratios versus Nd isotope ratios. Solid circles: U-IAT and open triangles: D-IAT. Primitive mantle value (M) and N-MORB value (N) are given in Table 2.

U-IAT have Nd isotope ratios which are close to the Bulk Earth value, and therefore are consistent with a model involving the primitive mantle as the source of U-IAT. In contrast, $^{87}Sr/^{86}Sr$ ratios of U-IAT range from 0.7047 to 0.7060, which are greater than or equal to the Bulk Earth value proposed by O'Nions *et al.* (1979). These variations could be caused by initial heterogeneity in Rb/Sr ratios of the primitive mantle as described below.

The Nd–Sr isotopic evolution of the Earth suggests that the Rb/Sr ratio of the primitive mantle is about one tenth while the Sm/Nd ratio

is the same as that of C1 chondrite (DePaolo and Wasserburg, 1976a). This difference between Rb/Sr and Sm/Nd ratios is caused mainly by the difference in the volatility of the elements during accretion of the Earth (Ganapathy and Anders, 1974). The large depletion in Rb relative to Sr may have resulted in Rb/Sr heterogeneity of the primitive mantle, which is estimated as varying from 0.029 to 0.038 with a ±15% variation range.

All currently available data on U-IAT are consistent with a model which suggests that the primary magma of U-IAT is derived by 5–10% partial melting of the primitive mantle.

A Two-Stage Model for D-IAT Magma Formation from the Primitive Mantle

D-IAT are characterized by convex-upward normalized patterns with a maximum value for an alkaline earth element in the NPR diagram (Fig. 5). The normalized values of LILE such as Cs, Rb, K and Ba increase with the decrease in ionic radii, and the variation in the degree of depletion of elements with large ionic radii is greater than the degree of depletion of elements with smaller ionic radii (Fig. 5). Since the D values of highly incompatible LILE do not decrease with the decrease in ionic radii of elements related to magma formation, the characteristics in Fig. 5 cannot be explained by different degrees of partial melting of a homogeneous mantle source (eq. (3) and (5), Fig. 8b) or by fractional crystallization(eq. (1) and (2), Fig. 8a), but only by a compositional variation in a mantle source (eq. (6), Fig. 8c).

The process of D-IAT formation can be explained by a two-stage model (eq. (7) and Fig. 9). The highest normalized value for incompatible elements in the two-stage model (eq. (7), Fig. 9) is close to that in a single-stage partial melting model (Fig. 8b), when the degrees of melting are similar, and when F′ is less than 0.01. The normalized value for Sr or Ba is the highest in the NPR diagram for D-IAT, and that value is close to the constant and high value observed for U-IAT. This fact implies that the F″ value of D-IAT is close to the F value of U-IAT (5–10%), and that F′ is less than 0.01. The D''_{Ba} value in this case is calculated to be 0.01 by eq. (8).

Assuming that D'_{Ba} and D''_{Ba} are 0.01, D′ for other incompatible elements in D-IAT can be calculated from eq. (9), when F′ is greater than 0.3% and F″ is 5–10%. The results show that D′ values are 0.0002 for Cs, 0.002 for Rb, and 0.008 for K of D-IAT from the Iwate volcano. It should be noted that D'_{La} needs to be one tenth of D''_{La} in the case of D-IAT. The low normalized value of La in D-IAT is due to the change in D during two-stages under different conditions. D'_{La} can be calculated to be 0.01, if D''_{La} is 0.1 which value is the same as D of La in U-IAT. The D''_{Y} in D-IAT can be calculated to be about 0.3 by eq. (8). This value is close to the D_Y value in U-IAT.

The good correlation between Nb/Y and Nd isotope ratios in Fig. 10 shows that the decrease in Nb/Y ratios is related to an increase in Sm/Nd ratios at some time, which was sufficiently old to have affected present-day Nd isotope ratios. A similar correlation is observed between Nd isotope and Zr/Y ratios of other subduction-related basalts (Ellam and Hawkesworth, 1988).

As shown in Fig. 11, a mantle isochron is obtained for Nd and Sm isotopes. The age of the isochron is 1.0±0.6 (2σ) Ga. The isochron for the depleted mantle which lost melt 1 Ga ago from the primitive mantle was estimated based on the method of DePaolo and Wasserburg (1976b, Fig. 11). The estimated mantle has a $^{147}Sm/^{144}Nd$ ratio higher than that observed in IAT. The difference can be explained as the effect of partial melting when the D''_{Sm} and D''_{Nd} are greater than 0.1 and D''_{Sm}/D''_{Nd} ratio is 1.2. These values are consistent with the preceding discussion for U-IAT.

From the above two-stage model for trace elements and Nd and Sr isotopes, it is concluded that the D-IAT magma formed in two-stage, consisting of a loss of a small amount of melt (<1%) from the primitive mantle about 1 Ga, and later 5–10% partial melting under the same condition as U-IAT.

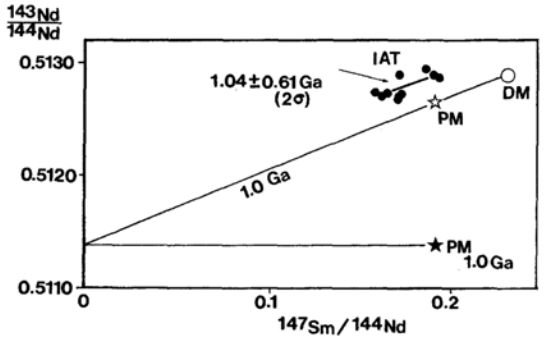

Fig. 11. "Isochron" plots of Nd–Sm isotopes for island arc tholeiite (IAT) from Northeast Japan arc. Data are from Table 1, except for one sample from Hachimantai after Masuda and Aoki (1979) and Nohda and Wasserburg (1981). The isochron shows an age of 1.0±0.6 (2σ) Ga. A mantle isochron is also shown for the case in which a melt was lost 1.0 Ga from the primitive mantle. There is a difference in $^{147}Sm/^{144}Nd$ between the IAT and that estimated for the source mantle [the depleted mantle (DM) and the primitive mantle (PM)]. It is explained by the compositional change of IAT derived from the source mantle by partial melting. See the text.

Separation of such a small amount of melt from the primitive mantle cannot be caused by extraction of viscous silicate melt, but rather by the removal of a low-viscosity melt (McKenzie, 1985). Therefore the estimated D′ for D-IAT should be of that between a volatile-rich melt and the residual mantle.

Geochemiscal Constraints on Island Arc Tholeiite Magma Genesis

Although U-IAT are a minority constituent of IAT, they play an important role to show the existence of a primitive mantle as a source of IAT. The rocks of U-IAT are found in the Iwate, Nasu and Adatara volcanoes in the volcanic front of Northeast Japan (Fig. 1). D-IAT constitute the majority of IAT and they can be found in most frontal volcanoes in Northeast Japan.

In our model, the existence of a primitive mantle together with a less than 1%-depleted one, under the Japanese island arc is required by the close relationship between trace elements and isotopes. It has been preserved under the island arc or continental crust from the effects of subduction, back arc mantle convection and past magmatism. A possibility of the existence of a primitive mantle in the oceanic and continental regions, termed the DUPAL anomaly, has been shown in the Southern Hemisphere on the basis of Sr, Pb and Nd isotope data (Dupré and Allègre, 1983, Hart, 1984, Hawkesworth *et al.*, 1986). For the Japan Arc, the possibility of a primitive or enriched mantle has been suggested only on the basis of Sr and Nd isotopic and/or major element compositions (Kagami *et al.*, 1986, Nohda *et al.*, 1988).

In our model, there is no need to add a subducted slab component to the source materials for IAT in order to explain their LILE and Sr and Nd isotopic composition. Only a very small amount of such a component is sufficient to explain the ^{10}Be and Pb isotopic anomalies shown in some arcs (Morris and Hart, 1986). Heat energy for the formation of the magma-bearing mush can be derived by upwelling of the high temperature part of the lower mantle induced by subduction (Ida, 1983, Kay and Kay, 1986).

Altered MORB or sea water cannot contribute to the low $^{143}Nd/^{144}Nd$ isotope ratios in IAT, because they have high Nd isotope ratios (O'Nions *et al.*, 1978). On the other hand, an addition of oceanic sediments, fluid extracted from the descending slab, including oceanic sediment (Nohda and Wasserburg, 1981) and/or continental crust, to the MORB source mantle has been offered as an alternative explanation for the Nd–Sr isotope ratios of IAT. However, as already mentioned, the correlation between Nb/Y and Nd isotope ratios of IAT shows that mantle heterogeneity cannot be derived by mixing of the N-MORB source mantle wedge and fluids extracted from subducted slab. In addition, elemental and isotopic data are not necessarily consistent with the mixing of oceanic sediments and/or continental crust. In the mixing models, most incompatible elements are derived from a contaminant (Ujike, 1988). Variations in the degrees of mixing and the composition of the contaminant would result in wide variations in

the composition of the source region. Moreover, oceanic sediments tend to have variable $^{143}Nd/^{144}Nd$ (Piepgras *et al.*, 1979), and continental crustal materials have a wide variation in elemental and isotopic compositions. Furthermore, according to the mixing models, U-IAT, which are enriched in LILE, should be mixed with more contaminant than D-IAT, and they should have a wider range of compositions. On the contrary, U-IAT from different volcanoes have uniform chemical composition and Nd isotope ratios. Thus, it is not easy to explain the genesis of IAT by the mixing models.

There is an inverse isotopic zonation between northeastern and central Japan as shown by Nohda and Wasserburg (1981) with the lack of any relationship between Sr enrichment and Sr isotopic ratios as shown by Arculus and Johnson (1981). Moreover, Sr concentrations of low-alkali tholeiite have restricted values. These facts are also incompatible with the simple mixing models.

The across-arc variation of alkaline concentrations and silica saturation can be explained by the difference in the depth of separation of magma from the mantle and by variations in the degree of partial melting (Tatsumi, 1983), rather than by differences in the composition of source materials. Na_2O+K_2O concentrations are sensitive to the degree of partial melting (F″) rather than the amount of melt lost in the residual mantle (F′) as shown in Fig. 9. In contrast, Rb/Sr ratios are strongly affected by the amount of melt lost in the residual mantle (F′), provided that F′ was small in Fig. 9. As a result, the alkali concentrations and $^{87}Sr/^{86}Sr$ ratios are not necessarily correlated in our model.

Acknowledgments—We especially thank M. Yagi, K. Matsumoto and other members of the Linac machine group of Laboratory of Nuclear Science, Tohoku University and M. Fujita and R. Yamadera of the RI center of Tohoku University for photon activation analyses. We thank K. Sato, University of Tokyo and J. Sato, Meiji University for analysis of Th by gamma ray spectrometry. We thank the late N. Onuma, Ibaraki University for analyzing Sr and Ba by ICP. We are grateful to H. Goto, H. Hattori, K. Shibata, T. Nakajima, S. Shirahase, H. Kamioka, and S. Uchiumi of the Geological Survey of Japan for assistance in XRF analysis and mass spectrometry and for stimulating discussions. We thank Y. Shimazaki, K. Uto and G. Caprarelli of the Geological Survey of Japan, S.-S. Sun of Bureau of Mines and Geology of Australia, R. W. Kay of Institute for Study of the Continent of Cornell University of U.S.A., C. J. Hawkesworth of Open University, U.K. and R. J. Arculus, University of New England, for the critical reading of this manuscript and for providing valuable suggestions.

References

Arculus, R. J. and Johnson, R. W. (1981) Island-arc magma sources: a geochemical assessment of the roles of slab-derived components and crustal contamination. *Geochem. J.* **15**, 109–133.

Arculus, R. J. and Powell, R. (1986) Source component mixing in the regions of arc magma generation. *J. Geophysic. Res.* **9**, B6, 5913–5929.

DePaolo, D. J. and Wasserburg, G. J. (1976a) Inferences about magma sources and mantle structure from variations of $^{143}Nd/^{144}Nd$. *Geophys. Res. Lett.* **3**, 743–746.

DePaolo, D. J. and Wasserburg, G. J. (1976b) Nd isotopic variations and petrogenetic models. *Geophys. Res. Lett.*, **3**, 249–252.

Dupré, B. and Allègre, C. J. (1983) Pb–Sr isotopic variation in Indian Ocean basalts a mixing phenomena. *Nature*, **303**, 142–146.

Ellam, R. M. and Hawkesworth, C. J. (1988) Elemental and isotopic variations in subduction related basalts: evidences for a three component model. *Contrib. Min. Petrol.* **98**, 72–80.

Frey, F. A. (1974) Atlantic oceanic floor: Geochemistry and petrology of basalt from Legs 2 and 3 of the Deep Sea Drilling Project. *J. Geophysic. Res.* **79**, 5507–5527.

Fujinawa, A. (1989) Tholeiitic and calc-alkaline magma series at Adatara volcano, Northeast Japan: 1 Geochemical constraints on their origin. *Lithos* **22**, 135–158.

Ganapathy, R. and Anders, E. (1974) Bulk compositions of the moon and earth, estimated from meteorites. *Proc. Fifth Lunar Sci. Conf.* **2**, 1181–1206.

Gill, J. (1981) Orogenic Andesites and Plate Tectonics. *Springer Verlag. Berlin.* pp. 390.

Green, T. H. and Pearson, N. J. (1985) Rare earth element partitioning between clinopyroxene and silicate liquid at moderate to high pressure, *Contrib. Mineral. Petrol*, **91**, 24–36.

Hart, S. R. (1984) A large-scale isotope anomaly in the Southern Hemisphere mantle. *Nature*. **309**, 753–757.

Hart, S. R. and Brooks, C. (1974) Clinopyroxene-matrix partitioning of K, Rb, Cs, Sr and Ba. *Geochim. Cosmochim. Acta*, **38**, 1799–1806.

Hawkesworth, C. J., Mantovani, M. S. M., Taylor, P. N. and Palacz, Z. (1986) Evidence from the Parana of south Brazil for a continental contribution to Dupal basalts. *Nature*. **322**, 356–359.

Hildreth, W. and Moorbath, S. (1988) Crustal contributions to arc magmatism in the Andes of Central Chile. *Contrib. Mineral. Petrol*. **98**, 455–489.

Ida, Y. (1983) Convection in the mantle wedge above the slab and tectonic process in subduction zones. *J. Geophys. Res*. **88**, 7449–7456.

Ishikawa, K. (1993) Petrology and geochemistry of the Iwate Volcano, northeastern Japan (in prep.).

Jakeš, P. and Gill, J. (1970) Rare earth elements and the island arc tholeiitic series. *Earth Planet. Sci. Lett*. **9**, 17–28.

Kagami, H., Iwata, M. and Takahashi, E. (1986) Isotope evidence for primitive mantle beneath the Sea of Japan, a young back arc basin. *Tech. Rep. ISEI, Okayama Univ. Ser. A*. No. 7, 1–13.

Kay, R. W. (1980) Volcanic arc magmas: Implications of a melting-mixing model for element recycling in the crust-upper mantle system. *J. Geol*. **88**, 497–522.

Kay, R. W. and Kay, S. M. (1986) Petrology and geochemistry of the lower continental crust: an overview. The nature of the lower continental crust, *Geol. Soc. Spec. Pub*. No. 24, 147–149.

Krahenbühl, U., Morgan, J. W., Ganapathy, R. and Anders, E. (1973) Abundance of 17 trace elements in carbonaceous chondrites. *Geochim. Cosmochim. Acta*. **37**, 1353–1370.

Kuno, H. (1966) Lateral variation of basalt magma type across continental margins and island arcs. *Bull. Volcanol*. **29**, 195–222.

Kurasawa, H., Fujinawa, A. and Leeman, W. P. (1986) Calc-alkaline rock series magmas coexisting within volcanoes in Japanese Island arcs-strontium isotopic study. *J. Geol. Soc. Japan*. **92**, 255–268 (in Japanese with English abstract).

Lugmair, G. W. and Carlson, R. W. (1978) The Sm-Nd history of KREEP. *Proc. Lunar Planet. Sci. Conf. 9th*, 689–704.

Masuda, A., Nakamura, N. and Tanaka, T. (1973) Fine structures of mutually normalized rare-earth patterns of chondrites. *Geochim. Cosmochim. Acta*. **37**, 239–248.

Masuda, Y. and Aoki, K. (1979) Trace element variations in the volcanic rocks from the Nasu zone, northeast Japan. *Earth, Planet Sci. Lett*. **44**, 139–149.

Matsuhisa, Y. (1979) Oxygen isotopic compositions of volcanic rocks from the East Japan island arcs and their bearing on petrogenesis. *J. Volcanol. Geotherm. Res*., **5**, 271–296.

Matsuhisa, Y. and Kurasawa, H.(1983) Oxygen and strontium isotope characteristics of calc-alkalic volcanic rocks from the central and western Japan arcs: evolution of contribution of crustal components to the magmas. *J. Volcanol. Geotherm. Res*. **18**, 483–510.

Matsui, Y., Onuma, N., Nagasawa, H., Higuchi, H. and Banno, S. (1977) Crystal structure control in trace element partition between crystal and magma, *Bull. Soc. fr. Mineral. Cristallogr*. **100**, 315–324.

McKenzie, D. (1985) The extraction of magma from the crust and mantle. *Earth. Planet. Sci. Lett*. **74**, 81–91.

Morris, J. D. and Hart, S. R. (1983) Isotopic and incompatible element constraints on the genesis of island arc volcanics from Cold Bay and Amak Island, Aleutians, and implications for mantle structure. *Geochim. Cosmochim. Acta*., **47**, 2015–2030.

Morris, J. D. and Hart, S. R. (1986) Isotopic and incompatible element constraints on the genesis of island arc volcanics from Cold Bay and Amak Island, Aleutians, and implications for mantle structure: Reply to a Critical Comment by M. R. Perfit And R. W. Kay. *Geochim. Cosmochim. Acta*. **50**, 483–487.

Nakamura, E., Campbell, I. H. and Sun, S. S. (1985) The influence of subduction processes on the geochemistry of Japanese alkaline basalts, *Nature*. **316**, 55–59.

Nichiporuk, W. and Moore, C. B. (1974) Lithium, sodium and potassium abundances in carbonaceous chondrites. *Geochim. Cosmochim. Acta*. **38**, 1691–1701.

Nicholls, I. A. and Ringwood, A. E. (1973) Effect of water on olivine stability in tholeiites and the production of silica saturated magmas in the island arc environment. *J. Geol*. **81**, 285–300.

Nohda, S. and Wasserburg, G. J. (1981) Nd and Sr isotopic study of volcanic rocks in Japan. *Earth Planet. Sci. Lett*. **52**, 264–276.

Nohda, S., Tatsumi, Y., Otofuji, Y., Matsuda, T. and Ishizaka, K. (1988) Asthenospheric injection and back-arc opening: isotopic evidence from northeast Japan. *Chem. Geol*. **68**, 317–327.

Notsu, K. (1983) Strontium isotope composition in volcanic rocks from the northeast Japan arc, *J. Volc. Geotherm*, Res. **18**, 531–548.

O'Nions, R. K., Carter, S. R., Cohen, R. S., Evensen, N. M. and Hamilton, P. J. (1978) Pb, Nd and Sr isotopes in oceanic ferromanganese deposits and ocean floor basalts. *Nature*. **273**, 435–438.

O'Nions, R. K., Carter, S. R., Evensen, N. M. and Hamilton, P. J. (1979) Geochemical and cosmochemical applications of Nd isotope analysis. *Ann. Rev. Earth Planet. Sci.* **7**, 11–38.

Perfit, M. R., Gust, D. A., Bence, A. E., Arculus, R. J. and Taylor, S. R. (1980) Chemical characteristics of island-arc basalts: implications for mantle sources. *Chem. Geol.* **30**, 227–256.

Perfit, M. R. and Kay, R. W. (1986) Comment on "Isotopic and incompatible element constraints on the genesis of island arc volcanics from Cold Bay and Amak Island, Aleutians, and implications for mantle structure" by J. D. Morris and S. R. Hart. *Geochim. Cosmochim: Acta.* **50**, 477–481.

Piepgras, D. J., Wasserburg, G. J. and Dasch, E. J. (1979) The isotopic composition of Nd in different ocean masses. *Earth. Planet. Sci. Lett.* **45**, 223–236.

Sakuyama, M. and Nesbitt, R. W. (1986) Geochemistry of the Quaternary volcanic rocks of the Northeast Japan arc. *J. Volc. Geotherm. Res.* **29**, 413–450.

Shannon, R. D. and Prewitt, C. T. (1969) Effective ionic radii in oxides and fluorides. *Acta Cryst. B25*, 925–945.

Shannon, R. D. and Prewitt, C. T. (1970) Revised values of effective ionic radii. *Acta Cryst. B26*, 1046–1048.

Stern, R. J. and Ito, E. (1983) Trace-element and isotopic constraints on the source of magmas in the active Volcano and Mariana island arcs, Western Pacific. *J. Volcanol. Geotherm. Res.* **18**, 461–482.

Sun, S. S. and Nesbitt, R. W. (1977) Chemical heterogeneity of the Archean mantle, composition of the earth and mantle evolution. *Earth. Planet. Sci. Lett.* **35**, 429–448.

Sun, S. S. and McDonough, W. F. (1989) Chemical and isotopic systematics of oceanic basalts: implications for mantle composition and process. *Magmatism in the Oceanic Basins, Geol. Soc. Spec. Publ. No. 42*, eds. Saunders, A. D. and Norry, M. J. 313–345.

Tatsumi, Y. (1983) Generation of arc basalt magmas and thermal structure of the mantle wedge in subduction zones. *J. Geophys. Res.* **88**, 5815–5825.

Tatsumi, Y., Hamilton, D. L. and Nesbitt, R. W. (1986) Chemical characteristics of fluid phase related from a subducted lithosphere and origin of arc magmas: evidence from high-pressure experiments and natural rocks. *J. Volcanol. Geotherm. Res.* **29**, 293–309.

Taylor, S. R. (1980) Refractory and moderately volatile element abundances in the earth, moon and meteorites. *Proc. Lunar Planet. Sci. Conf. 11th*, 333–348.

Ujike, O. (1988) Probable mineralogic control on the mantle metasomatic fluid composition beneath the Northeast Japan arc. Geochim. Cosmochim. Acta. **52**, 2037–2046.

White, W. M. and Hofmann, A. W. (1982) Sr and Nd isotope geochemistry of oceanic basalts and mantle evolution, *Nature*, **296**, 821–825.

Wood, D. A., Joron, J. L., Treuil, M., Norry, M. and Tarney, J. (1979) Elemental and Sr isotope variations in basic lavas from Iceland and the surrounding ocean floor. *Contrib. Mineral. Petrol.* **70**, 319–339.

Yoshida, T., Matsumoto, K. and Aoki, K. (1986) Photon activation analysis of standard rocks using an automatic γ-ray counting system with a micro-robot. *J. Japan. Assoc. Min. Pet. Econ. Geol.* **81**, 406–422.

Yoshida, T. and Aoki, K. (1984) Geochemistry of major and trace elements in the Quaternary volcanic rocks from northeast Honshu, Japan. *Sci. Rep. Tohoku. Univ. Ser. III*, **16**, 1–34.